Materials Today: Proceedings xxx (xxxx) xxx

Contents lists available at ScienceDirect

Materials Today: Proceedings

journal homepage: www.elsevier.com/locate/matpr

Fabrication of micro and nanostructures on glass using non-isothermal thermal imprinting

Raja Murfiqah binti Raja Mohamad Fouzy, Norfazilasari binti Yasman, Mohd Zairulnizam bin Mohd Zawawi *

Faculty of Manufacturing and Mechatronic Engineering Technology, Universiti Malaysia Pahang, 26600 Pekan, Pahang, Malaysia

ARTICLE INFO

Keywords:
Thermal imprinting
Non-Isothermal
Optical glass
Microlens Array (MLA)
Nanostructures

ABSTRACT

The formation of micro/nano scale pattern features on glass using direct thermal imprinting has gained continuous attention due to its potential to replicate glass with various functional surfaces at an atomic scale resolution. Unfortunately, the long thermal cycle issue in regular thermal imprinting remains the main obstacle that hampered the process to be viable for mass production. In this paper, the fabrication of micro/nano scale pattern features directly on glass substrate using non-isothermal thermal imprinting is proposed. Compared to conventional thermal imprinting, this method eliminates the serial process of heating, soaking, pressing, demolding, and cooling that commonly took place in one close chamber. Therefore, the duration of each imprinting cycle is significantly decreased, which in turn could reduce the cost per unit price to fabricate these glass devices with micro and nanostructures. The morphology of these imprinted glass nanograting and microlens array (MLA) was characterized via the scanning electron microscope (SEM), atomic force microscope (AFM) and surface profiler. Overall, the imprinted nanograting and MLA pattern using the non-isothermal thermal imprinting method result showed good replication fidelity, comparable to the regular thermal imprinting and outperforms the conventional one in terms of overall cycle time reduction, minimized variation of mold temperature and lower energy consumption. The proposed method is expected to become an interesting approach for fabrication of various patterns directly on glass substrate with high pattern quality and shorter thermal cycle.

1. Introduction

Nowadays, glass based optical components with various micro-nanostructures features are becoming prominent in optical applications where high thermal stability, excellence transmittance in the ultraviolet (UV) region, high durability and superior optical performance are necessary. Due to the growing demand for miniaturization devices in a wide range of industries, researchers have devoted a significant amount of effort to develop new glass-based devices as well as improving the process efficiency. The numerous potential applications include optical imaging [1,2], microfluidics [3,4], sensors [5,6], illumination [7] and fiber coupling [8,9]. A wide variety of well-established micro-nano fabrication methods have been practiced in the industry and continuously investigated by the academia. These include micro-injection molding [10], thermal reflow [11,12], photolithography [13], nano imprinting [14–16], laser structuring [17,18], direct imprinting [19–21] and hot embossing [22,23].

Photolithography has been successful for a long time as a micro-patterning method on various substrate processes with great homogeneity, precise geometrical shape, optics surface finish, and excellence repeatability. Nevertheless, the photolithography procedure necessitates a costly and sophisticated setup to complete the patterning process. Furthermore, this process requires an expensive photomask, limited resolution, and multiple steps which are only suitable for fabrication of master mold template. Meanwhile, laser structuring is another interesting direct patterning approach for fabrication of micro/nano features [24]. Unfortunately, the process requires a secondary process such as heat treatment, etching and cleaning due to the ablated material in the form of debris and poor pattern uniformity after the laser scanning process. Polymer based micro-devices could be produced by injection molding process with numerous advantages such as one single production step, low production cost and complex shape. Despite that, this

* Corresponding author.
E-mail address: zairulnizam@ump.edu.my (M.Z.M. Zawawi).

https://doi.org/10.1016/j.matpr.2023.08.181
Received 24 June 2023; Received in revised form 14 August 2023; Accepted 17 August 2023

Please cite this article as: Raja Murfiqah binti Raja Mohamad Fouzy et al., *Materials Today: Proceedings*, https://doi.org/10.1016/j.matpr.2023.08.181

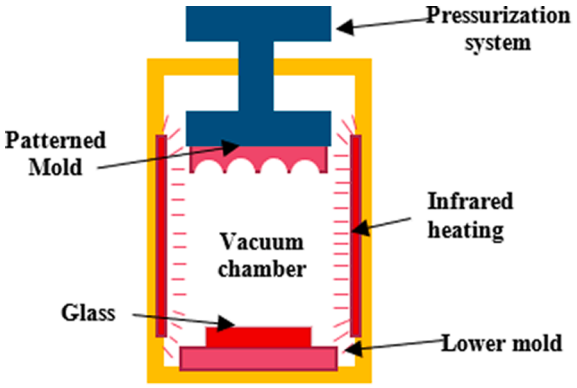

Fig. 1. Schematic of conventional isothermal thermal imprinting.

replication process is limited to polymer material and difficult to produce molded parts of micro/nano features with high aspect ratio. Surface tension driven methods such as thermal reflow are other notable processes for formation of microlens array pattern of various profile with high uniformity and good optics quality. However, the overall process cycle time was long that consisted of photoresist coating, UV exposure, development, and very sensitive time-dependent heating control. One inherent problem is the difficulty of controlling the contact angle due to the wettability effect from the substrate itself and its surrounding air.

Thermal imprinting or so-called hot embossing is one promising replication method for the mass production of optical elements with micro-nano patterns due to its prominent benefits of simple and cost-effective setup. This method was extended from an earlier process called precision glass molding; used for manufacturing glass lenses. Overall, once a precise and durable coated mold has been fabricated, it can be used repeatedly to replicate sub-micron feature size on various substrate surface including glass, polymer, and metal without any secondary or subsequent treatment. Nonetheless, the existing isothermal glass thermal imprinting process and its nature of configuration resulted in long thermal cycle, generally could not be less than 20 min and might be an hourly process depending on the glass material properties, pattern feature size, shape, duty ratio and aspect ratio. The process consists of heating, soaking, pressing, demolding, and cooling that took place in serial manners inside one close chamber. In addition, the mold temperature variations in each molding cycle were large which in turn accelerates the molds wear after long use. To improve the production efficiency of the regular glass molding process, non-isothermal glass molding of spherical and aspherical lens had been demonstrated [25]. However, these non-isothermal glass molding use closed -mold design and did not involve replication of fine pattern features.

In this work, fabrication of fine micro/nano scale pattern features directly on glass substrate using non-isothermal thermal imprinting is proposed. In this new configuration, the glass was preheated externally on a conveyor, then moved to the imprinting station for pattern transfer, demolding, and external cooling. The morphology of these imprinted glass nanograting and microlens array (MLA) was characterized via the scanning electron microscope (SEM), atomic force microscope (AFM) and three-dimensional (3D) laser scanning confocal microscope (LSCM).

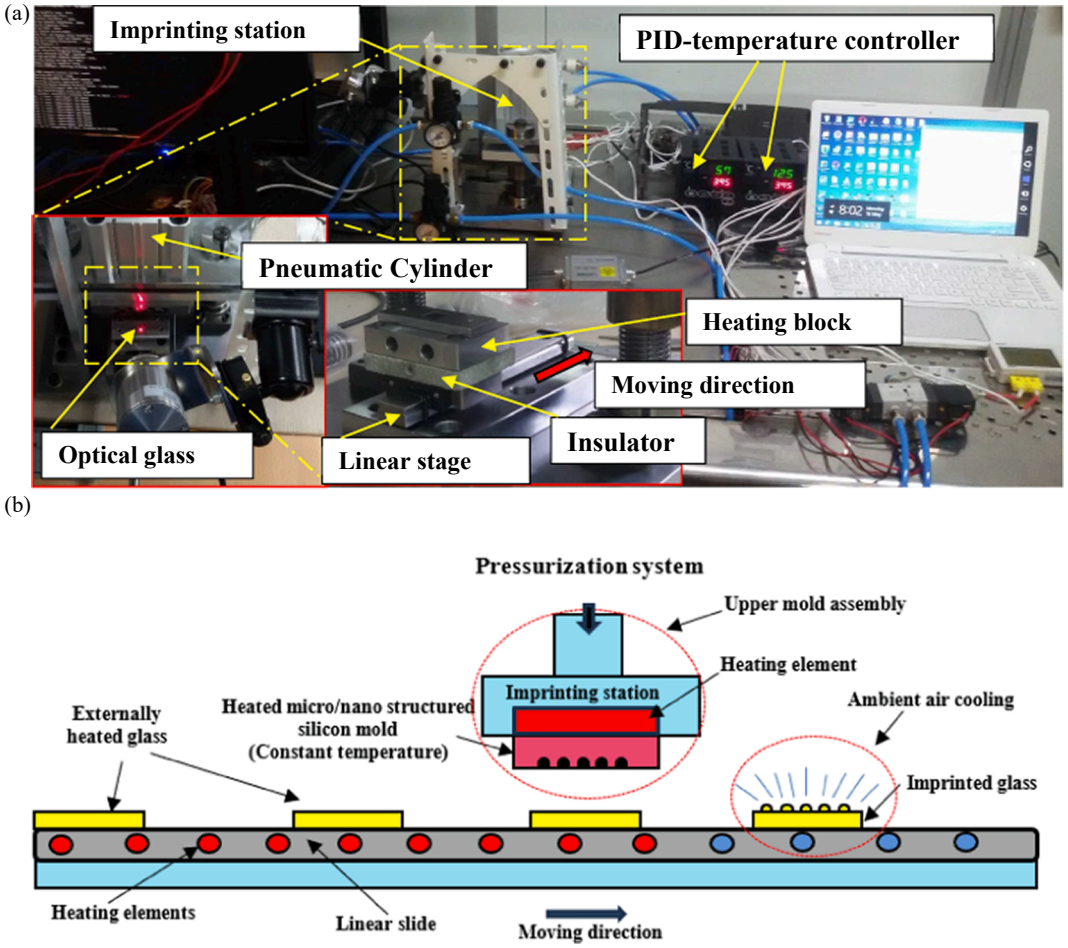

Fig 2. (a) Photo image of the actual non-isothermal thermal imprinting experimental setup, (b) schematic of non-isothermal thermal imprinting.

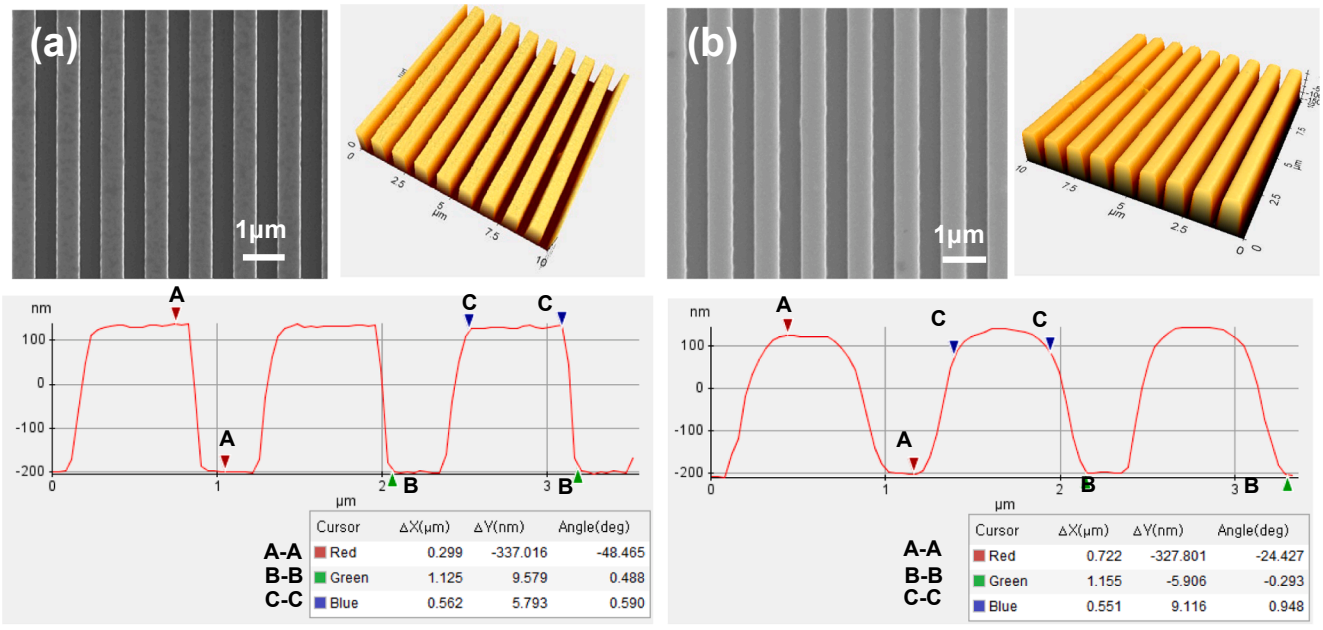

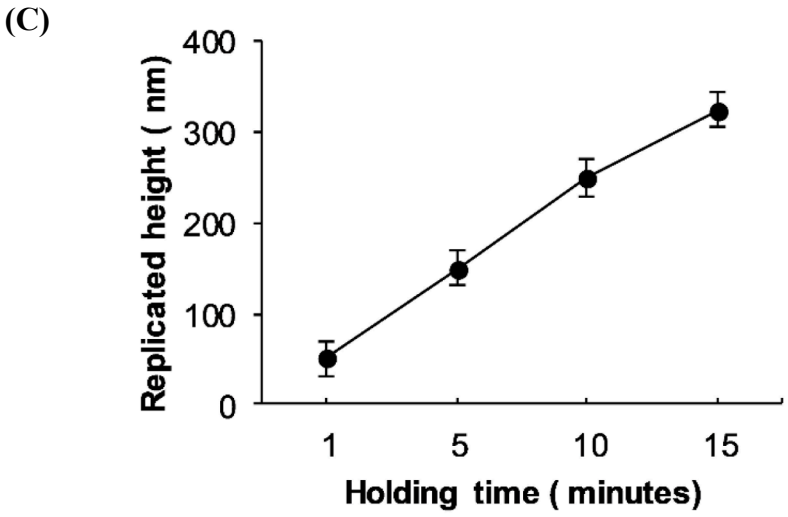

Fig. 3. (a) Top view sem image (left), afm 3d image (right) and afm 2d profile of the silicon mold (bottom), (b) top view sem image (left), afm 3d image (right) and afm 2d profile of the imprinted glass (bottom), (c) replication height as a function of different holding time of the 550 nm L/S pattern (Imprinting temperature of 365 °C, constant pressure of 4 MPa).

2. Material and experimental setup

K-PG375 optical glass (Sumita Optical Glass Inc., Saitama, Japan); with a glass transition temperature (T_g) of 344 °C and a yield temperature (A_t) of 367 °C was used as the substrates in the experiment. Two types of patterns were used; nanoscale features consist of periodic line and space pattern (L/S) of 550 nm (~335 ± 20 nm height) and microscale features comprises of concave MLA pattern with diameter of 80 μm, pitch of 100 μm, and sag height average of 14.8 ± 0.3 μm. The former master stamp material was silicon; fabricated via well-established semiconductor processing technology consists of photoresist coating, Krypton-fluoride (KrF) scanning lithography followed by reactive ion etching (RIE). The latter mold material was nickel, manufactured by photolithography, thermal reflow, nickel seed layer evaporation and electroforming on a silicon master. To minimize adherence of the glass material to the mold during the thermal imprinting process, the silicon mold was coated with 40 nm thick silicon nitride while the nickel mold was coated with 1 μm thick diamond like carbon (DLC). For brief comparison, Fig. 1 illustrates the schematic of the conventional isothermal thermal imprinting setup. First, infrared heating was used to simultaneously heat the glass, the patterned mold as well as the flat lower mold to the desired temperature. Sufficient soaking time is then given to ensure a uniform temperature. This is then followed by pressing at certain holding time, demolding, and cooling inside the closed vacuum chamber.

To investigate the applicability of the proposed technique, non-isothermal glass thermal imprinting experiments were carried out using a home built thermal imprinting system. Fig. 2(a) shows the photo image of the actual non-isothermal thermal imprinting experimental setup, and Fig. 2(b) shows the schematic of non-isothermal thermal

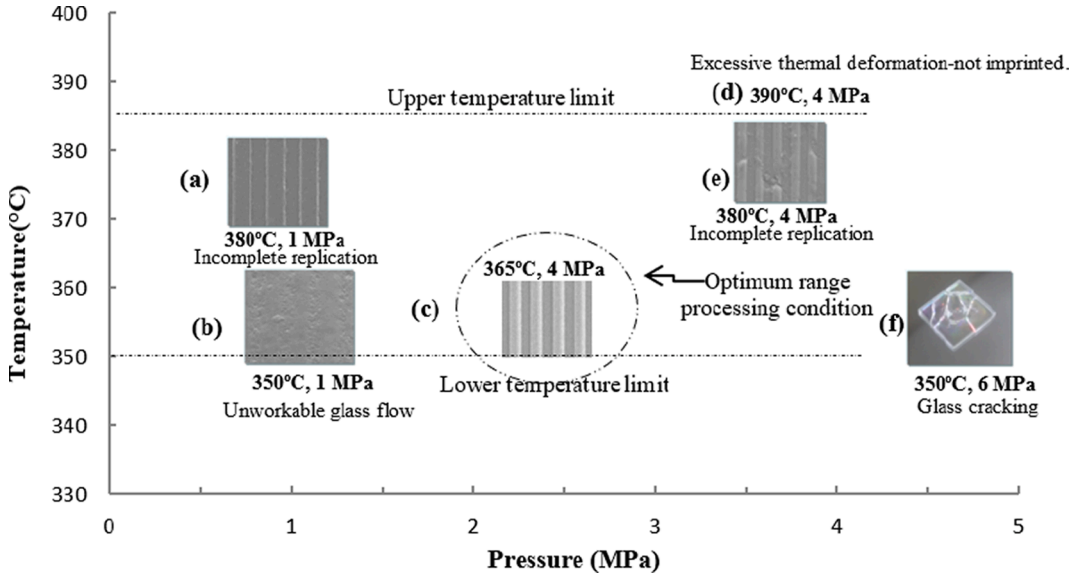

Fig. 4. General processing characteristics in conventional thermal imprinting.

imprinting which was used in the experiment. Once the externally heated glass was transferred to the imprinting station, the upper mold assembly which contains the nanostructured mold gradually lowered down and made a pressing contact with the glass. After demolding, the linear slide that carried the glasses was externally cooled to room temperature via ambient air and assistance from cooling fan. This configuration eliminates the serial process of heating, soaking, pressing, demolding, and cooling that commonly took place in one close chamber. Therefore, the duration of each imprinting cycle is significantly decreased.

3. Results and discussion

3.1. Non-isothermal thermal imprinting of nanoscale pattern result

The left Fig. 3(a) shows the top view SEM image of the silicon mold which consists of periodic nanograting pattern of 550 nm L/S (~335 ± 20 nm height). Fig. 3(a)-right and Fig. 3(a)-bottom shows the AFM-3D image and AFM-2D cross-section measurement. The SEM image of the imprinted glass, AFM-3D and AFM-2D are shown in Fig. 3(b)-left, Fig. 3 (b)-right and Fig. 3(b)-bottom, respectively. The glass was imprinted at temperature of 365 °C, constant pressure of 4 MPa and holding time of 15 minutes. Using these parameters, the glass pattern replication height reached ~327 nm (90% filling height), slightly lower than the mold pattern height with rounded shape at the corner. Even though the

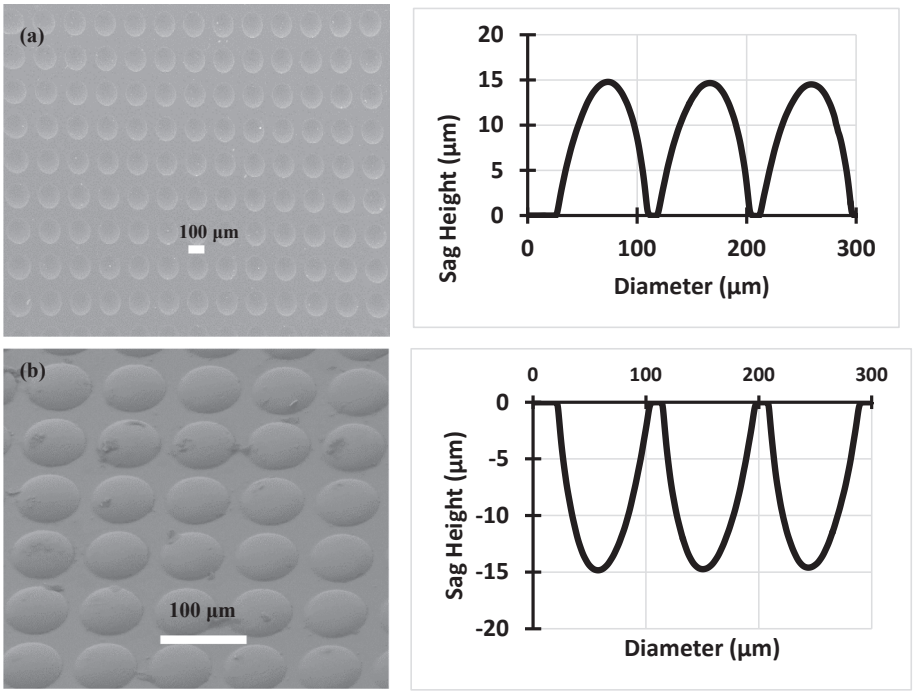

Fig. 5. (a) SEM image of the 80 µm diameter of nickel mold of MLA's (left) and 2D surface profiler measurement of the nickel mold (right) (b) SEM image of the imprinted glass of 80 µm diameter MLA's (left) and 2D surface profiler measurement of the imprinted glass (right).

perfect inverse shape from the mold was transcribed on the glass surface, the quality was acceptable since the replicated pattern width and pitch closely match the mold. Furthermore, there is no sign of pattern damage indicating that the K-PG375 glass was successfully demolded. The difficulty to obtain complete replication for pattern feature of below 1 μm had been reported by previous study [26–28]. Based on the AFM measurement, the measured average surface roughness of the silicon mold and the corresponding imprinted glass nanograting was about 0.66 nm and 2.59 nm, respectively. The replication height may be improved if either slight increase of molding temperature, longer pressing contact time or higher pressing load were used. The incomplete filling may be attributed to several factors. First, the small size of the grating cavity poses a greater difficulty for the thermal imprinting process, as it becomes more challenging for the molten material to flow into all the intricate features of the nanograting. The limited space within the small grating cavity restricts the material flow and hinders complete filling of the pattern. Fig. 3(c) shows the relationship between the replicated 550 nm L/S grating heights at different holding time. The holding time for each imprinting test was 1 min, 5 min, 10 min, and 15 min in which the respective pattern replication heights were measured by AFM. Clearly, as the holding time increases, the replicated height also increases. We should mention here that our current non-isothermal thermal imprinting setup was not performed in a vacuum chamber. This condition may induce an air bubble and oxidation which make it very difficult to obtain a perfect pattern transfer. We believed that with a slight optimization in the processing parameters and the incorporation of the whole system in a closed vacuum chamber will improve the flowability of the glass material onto the nanostructured mold cavities.

It is noteworthy to mention that the range of acceptable thermal imprinting process parameters do exist which not only determine the quality of the pattern transfer, but also affect both the thickness reduction of the glass and cracking. Fig. 4 illustrates general characteristics of non-isothermal direct glass thermal imprinting at different temperature and pressing load, which was observed during the optimization trials. Particularly, the process was sensitive to temperature. Overall, we found that the processing window to achieve fine imprinting quality is quite narrow (Inset Fig. 4(c)). Even though ideally the increase of imprinting temperature will reduce the glass viscosity as well as enhancing the filling ratio, it is rather limited to a certain temperature range. For instance, imprinting at temperature of above the glass at such as 370 °C and above resulted in poor pattern quality and further deteriorates as the temperature increase until no pattern transfer was visible. This condition occurred because the glass was too soft and resulted in high thermal deformation of the glass under pressing load (Inset Fig. 4(d)). Meanwhile, the glass was still hard at temperature of slightly above the glass T_g such as 350 °C, resulted in low formability (Inset Fig. 4(b)), incomplete glass filling (Inset Fig. 4(a)) or glass cracking (Inset Fig. 4(f)).

3.2. MLA's pattern thermal imprinting result

Apart from thermal imprinting of nanoscale features, the imprinting of microscale pattern was also attempted. The left Fig. 5(a) shows the top view SEM image of the nickel mold which consist of MLA pattern with diameter of 80 μm, pitch of 100 μm, and sag height average of 14.8 ± 0.3 μm. Fig. 5(a)-right shows its 2D cross-section as measured by the surface profiler. The SEM image of the imprinted glass MLA pattern and 2D surface profiler result is depicted in Fig. 5(a) and Fig. 5(b), respectively. The non-isothermal thermal imprinting was conducted at an imprinting temperature of 365 °C, a pressing load of 2 MPa, and a holding time of 150 s. The measured average surface roughness of the 5 μm × 5 μm square area at the top surface of the imprinted glass MLA was about 8.948 nm. The results revealed that the inverse pattern from the nickel stamp was finely transferred to the glass surface, demonstrating a high level of replication fidelity. The measured sag height average of the imprinted glass MLA was about 14.6 ± 0.3 μm, slightly lower than the

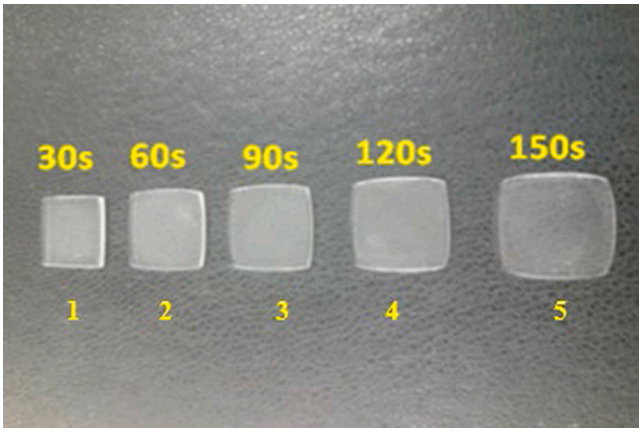

Fig. 6. Photo image of the imprinted glass MLA sample after different holding time (From left to right- 30 s, 60 s, 90 s, 120 s and 150 s).

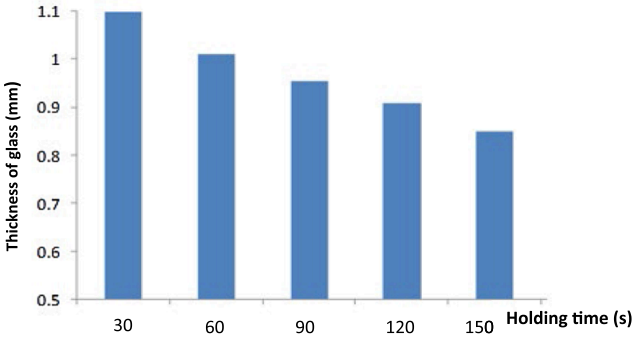

Fig. 7. The corresponded final glass substrate thickness after different holding time (Constant imprinting temperature of 370 °C and imprinting pressure of 4 MPa).

master mold. Therefore, it is fair to say that the glass does shrink after the demolding and cooling process. Up to this stage, it is evident that the non-isothermal thermal imprinting approach employed in this study could achieve excellent replication results both for nanoscale and microscale features. Like what was observed during thermal imprinting of glass nanograting, MLA sag height increased as the imprinting temperature and holding time were raised. This outcome was expected, as the viscosity of the glass decreased with higher imprinting temperatures. The reduction in glass viscosity facilitated the flow of the glass material onto the mold during the thermal imprinting process, thereby resulting in an increase in sag height.

The incomplete fill of the nanograting pattern described in Section 3.2 can be attributed to the smaller size of the grating cavity. The reduced dimensions pose a greater difficulty for the thermal imprinting process, as it becomes more challenging for the molten material to flow into all the intricate features of the nanograting. The limited space within the small grating cavity restricts the material flow and hinders complete filling of the pattern. To address this issue and achieve satisfactory replication of the nanograting pattern, higher holding times and pressures are necessary compared to those used for the microlens array pattern. The increased holding time allows for better material flow and helps ensure that the molten material can reach and fill all the corners and recesses of the nanograting. Similarly, higher pressures facilitate more effective material flow and ensure that the pattern is replicated with greater accuracy.

3.3. Final glass substrate thickness reduction

While the increase of molding temperature, holding time, and

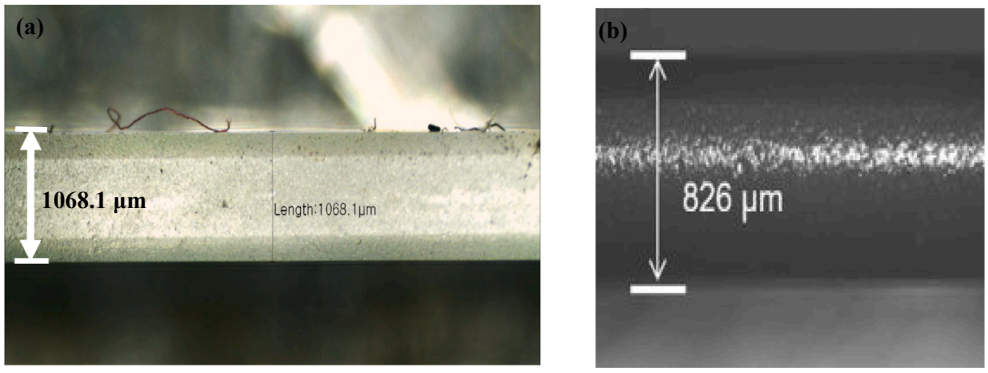

Fig. 8. The measured optical glass thickness (a) before imprint, (b) after imprinting holding time of 150 s.

pressure can enhance the flow of the glass onto the micro/nano-structured cavities during the thermal imprinting process, the effect of these parameters to the final glass substrate thickness should not be neglected. It is crucial to avoid excessive thickness reduction, which can negatively affect the functionality of the final parts, particularly when it comes to assembly or integration with other components. Fig. 6 shows the top view photo image of the imprinted glass MLA after different holding time (30 s, 60 s, 90 s, 120 s and 150 s). Obviously, lateral thermal deformation expanded the final area of the glass. Fig. 7 shows the corresponded final glass substrate thickness after different holding time as measured by optical microscope. Obviously, the glass thickness reduced as the holding time increased. Fig. 8(a) shows the raw glass thickness before the thermal imprinting while Fig. 8(b) shows one example of the measured final imprinted glass after holding time of 150 s. We then further confirm the uniformity of the imprinted glass compared to the raw glass material where surface profiler was used to measure across the 7 mm distance of the glass surface. The surface roughness value R_z of the raw glass material and the imprinted glass were about 6 nm and 24 nm, respectively. Therefore, striking a balance between achieving desired pattern replication height and maintaining the structural integrity of the glass parts is of utmost importance.

4. Conclusion

The fabrication of micro and nanostructures on glass using a non-isothermal thermal imprinting process has been demonstrated. Clearly, this approach can achieve high-quality micro/nano structure patterns, comparable to those obtained through conventional isothermal thermal imprinting methods. We successfully replicated nanoscale pattern from the silicon mold; periodic nanograting pattern of 550 nm L/S (~335 ± 20 nm height) to the glass surface which attain 90% filling height. In addition, the inverse pattern from the nickel stamp was also finely transferred to the glass surface with high level of replication fidelity. The measured sag height average of the imprinted glass MLA was about 14.6 ± 0.3 µm, slightly lower than the master mold sag height average of 14.8 ± 0.3 µm. Overall, the imprinted nanograting and MLA pattern using the non-isothermal thermal imprinting method results showed good replication fidelity, comparable to the regular thermal imprinting and outperforms the conventional one in terms of overall cycle time reduction, minimized variation of mold temperature and lower energy consumption. We believed that the quality of the replicated pattern could be further improved if the whole system was incorporated in a closed vacuum chamber; eliminates air bubble and oxidation which in turns can improve the flowability of the glass material onto the nanostructured mold cavities. Even though in this study only K-PG375 optical glass was used, we believed that other types of optical glass could also be used in the proposed non-isothermal thermal imprinting. The attempt on other types of glass including the integration of the system with vacuum chamber is the subject of our ongoing research. The proposed method is expected to become an interesting approach for fabrication of various patterns directly on glass substrate with high pattern quality and shorter thermal cycle.

CRediT authorship contribution statement

Norfazilasari binti Yasman: Methodology, Investigation.

Declaration of Competing Interest

The authors declare that they have no known competing financial interests or personal relationships that could have appeared to influence the work reported in this paper.

Data availability

Data will be made available on request.

Acknowledgements

This research was supported by Internal Fundamental Research Grant with the grant number RDU220301, Universiti Malaysia Pahang (UMP).

References

[1] F. Yang, W. Yan, P. Tian, F. Li, F. Peng, Electro-optical imaging technology based on microlens array and fiber interferometer, Appl. Sci. (Switzerland) 9 (7) (2019), https://doi.org/10.3390/app9071331.
[2] J.W. Duparre, P. Schreiber, P. Dannberg, T. Scharf, P. Pelli, R. Voelkel, H.-P. Herzig, A. Braeuer, Artificial compound eyes: different concepts and their application for ultraflat image acquisition sensors, MOEMS Miniaturized Syst. IV 5346 (2004) 89, https://doi.org/10.1117/12.530208.
[3] S.K. Tiwari, S. Bhat, K.K. Mahato, Design and fabrication of low-cost microfluidic channel for biomedical application, Sci. Rep. 10 (1) (2020), https://doi.org/10.1038/s41598-020-65995-x.
[4] J. Zhou, A. Kulasinghe, A. Bogseth, K. O'Byrne, C. Punyadeera, I. Papautsky, Isolation of circulating tumor cells in non-small-cell-lung-cancer patients using a multi-flow microfluidic channel, Microsyst. Nanoeng. 5 (1) (2019), https://doi.org/10.1038/s41378-019-0045-6.
[5] H.M. Kim, M.S. Kim, G.J. Lee, H.J. Jang, Y.M. Song, Miniaturized 3D depth sensing-based smartphone light field camera, Sensors (Switzerland) 20 (7) (2020), https://doi.org/10.3390/s20072129.
[6] S. Li, Y. Yuan, Z. Gao, H. Tan, High-accuracy correction of a microlens array for plenoptic imaging sensors, Sensors (Switzerland) 19 (18) (2019), https://doi.org/10.3390/s19183922.
[7] R. Datt, H.K.H. Lee, M. Spence, M. Carnie, W.C. Tsoi, High performance non-fullerene organic photovoltaics under implant light illumination region, Appl. Phys. Lett. 122 (14) (2023), https://doi.org/10.1063/5.0144861.
[8] H. Zhou, H. Xu, J.A. Duan, Review of the technology of a single mode fiber coupling to a laser diode, Opt. Fiber Technol. 55 (2020), https://doi.org/10.1016/j.yofte.2019.102097.
[9] T. Watanabe, Y. Fedoryshyn, J. Leuthold, 2-D grating couplers for vertical fiber coupling in two polarizations, IEEE Photonics J. 11 (4) (2019), https://doi.org/10.1109/JPHOT.2019.2926823.

[10] F. Fang, N. Zhang, X. Zhang, Precision injection molding of freeform optics, in: Advanced Optical Technologies, Walter de Gruyter GmbH, 2016, pp. 303–324. https://doi.org/10.1515/aot-2016-0033.
[11] H. Xiong, Z. Wang, Fabrication of ternary Ge-Se-Sb chalcogenide microlens arrays using thermal reflow, J. Micromech. Microeng. 29 (8) (2019), https://doi.org/10.1088/1361-6439/ab1e61.
[12] J.Y. Tan, G. Goh, J. Kim, Microfabrication of microlens by timed-development-and-thermal-reflow (TDTR) process for projection lithography, Micromachines 11 (3) (2020), https://doi.org/10.3390/mi11030277.
[13] M.-H. Wu, G.M. Whitesides, Fabrication of two-dimensional arrays of microlenses and their applications in photolithography, Inst. Phys. Publ. J. Micromech. Microeng. 12 (2002). http://iopscience.iop.org/0960-1317/12/6/305.
[14] P. Yi, H. Wu, C. Zhang, L. Peng, X. Lai, Roll-to-roll UV imprinting lithography for micro/nanostructures, J. Vac. Sci. Technol., B: Nanotechnol. Microelectron.: Mater., Process., Meas., Phenom. 33 (6) (2015), 060801, https://doi.org/10.1116/1.4933347.
[15] S. Tzadka Shalit, N. Ostrovsky, H. Frankenstein Shefa, E. Kassis, S. Joseph, M. Schvartzman, Direct nanoimprint of chalcogenide glasses with optical functionalities via solvent-based surface softening, Opt. Express 30 (15) (2022) 26229, https://doi.org/10.1364/oe.462448.
[16] M. Lotz, J. Needham, M.H. Jakobsen, R. Taboryski, Nanoimprinting reflow modified moth-eye structures in chalcogenide glass for enhanced broadband antireflection in the mid-infrared, Opt. Lett. 44 (17) (2019) 4383, https://doi.org/10.1364/ol.44.004383.
[17] R. Li, C. Li, M. Yan, M. Li, C. Lin, S. Dai, B. Song, T. Xu, P. Zhang, Fabrication of chalcogenide microlens arrays by femtosecond laser writing and precision molding, Ceram. Int. (2023), https://doi.org/10.1016/j.ceramint.2023.01.181.
[18] C.H. Lin, L. Jiang, Y.H. Chai, H. Xiao, S.J. Chen, H.L. Tsai, Fabrication of microlens arrays in photosensitive glass by femtosecond laser direct writing, Appl. Phys. A Mater. Sci. Process. 97 (4) (2009) 751–757, https://doi.org/10.1007/s00339-009-5350-8.
[19] N. Ostrovsky, D. Yehuda, S. Tzadka, E. Kassis, S. Joseph, M. Schvartzman, Direct imprint of optical functionalities on free-form chalcogenide glasses, Adv. Opt. Mater. 7 (19) (2019), https://doi.org/10.1002/adom.201900652.
[20] S. Tzadka, N. Ostrovsky, E. Toledo, G.L. Saux, E. Kassis, S. Joseph, M. Schvartzman, Surface plasticizing of chalcogenide glasses: a route for direct nanoimprint with multifunctional antireflective and highly hydrophobic structures, Opt. Express 28 (19) (2020) 28352, https://doi.org/10.1364/oe.400038.
[21] C. Ye, G.J. Cheng, Scalable patterning on shape memory alloy by laser shock assisted direct imprinting, Appl. Surf. Sci. 258 (24) (2012) 10042–10046, https://doi.org/10.1016/j.apsusc.2012.06.070.
[22] N. Jürgensen, B. Fritz, A. Mertens, J.N. Tisserant, M. Kolle, G. Gomard, G. Hernandez-Sosa, A single-step hot embossing process for integration of microlens arrays in biodegradable substrates for improved light extraction of light-emitting devices, Adv. Mater. Technol. 6 (2) (2021), https://doi.org/10.1002/admt.201900933.
[23] N.S. Ong, Y.H. Koh, Y.Q. Fu, Microlens array produced using hot embossing process, Microelectron. Eng. 60 (2002).
[24] H.P. Wang, Y.C. Guan, H.Y. Zheng, M.H. Hong, Controllable fabrication of metallic micro/nano hybrid structuring surface for antireflection by picosecond laser direct writing, Appl. Surf. Sci. 471 (2019) 347–354, https://doi.org/10.1016/j.apsusc.2018.11.245.
[25] C. Ye, G.J. Cheng, Scalable patterning on shape memory alloy by laser shock assisted direct imprinting, Appl. Surf. Sci. 258 (24) (2012) 10042–10046, https://doi.org/10.1016/j.apsusc.2012.06.070.
[26] K. Li, G. Xu, X. Liu, F. Gong, Deformation behavior of glass nanostructures in hot embossing, ACS Appl. Mater. Interfaces 12 (32) (2020) 36311–36319, https://doi.org/10.1021/acsami.0c08435.
[27] Y.M. Hung, Y.J. Lu, C.K. Sung, Microstructure patterning on glass substrate by imprinting process, Microelectron. Eng. 86 (4–6) (2009) 577–582, https://doi.org/10.1016/j.mee.2009.02.015.
[28] M.R. Lotz, C.R. Petersen, C. Markos, O. Bang, M.H. Jakobsen, R. Taboryski, Direct nanoimprinting of moth-eye structures in chalcogenide glass for broadband antireflection in the mid-infrared, Optica 5 (5) (2018) 557, https://doi.org/10.1364/optica.5.000557.